ResearchGate

See discussions, stats, and author profiles for this publication at: https://www.researchgate.net/publication/237095354

Air Quality Impact and Physicochemical Aging of Biomass Burning Aerosols during the 2007 San Diego Wildfires

ARTICLE *in* ENVIRONMENTAL SCIENCE & TECHNOLOGY · JUNE 2013

Impact Factor: 5.33 · DOI: 10.1021/es4004137 · Source: PubMed

CITATIONS
12

READS
24

5 AUTHORS, INCLUDING:

Kim Prather
University of California, San Diego
297 PUBLICATIONS **9,860** CITATIONS

SEE PROFILE

Available from: Kim Prather
Retrieved on: 03 February 2016

Environmental Science & Technology

Article

pubs.acs.org/est

Air Quality Impact and Physicochemical Aging of Biomass Burning Aerosols during the 2007 San Diego Wildfires

Melanie D. Zauscher,[†,∥] Ying Wang,[‡,⊥] Meagan J. K. Moore,[‡,#] Cassandra J. Gaston,[§,▽] and Kimberly A. Prather*[,‡,§]

[†]Department of Mechanical and Aerospace Engineering, University of California, San Diego, California

[‡]Department of Chemistry and Biochemistry, University of California, San Diego, California

[§]Scripps Institution of Oceanography, University of California, San Diego, California

Supporting Information

ABSTRACT: Intense wildfires burning >360 000 acres in San Diego during October, 2007 provided a unique opportunity to study the impact of wildfires on local air quality and biomass burning aerosol (BBA) aging. The size-resolved mixing state of individual particles was measured in real-time with an aerosol time-of-flight mass spectrometer (ATOFMS) for 10 days after the fires commenced. Particle concentrations were high county-wide due to the wildfires; 84% of 120−400 nm particles by number were identified as BBA, with particles <400 nm contributing to mass concentrations dangerous to public health, up to 148 $\mu g/m^3$. Evidence of potassium salts heterogeneously reacting with inorganic acids was observed with continuous high temporal resolution for the first time. Ten distinct chemical types shown as BBA factors were identified through positive matrix factorization coupled to single particle analysis, including particles comprised of potassium chloride and organic nitrogen during the beginning of the wildfires, ammonium nitrate and amines after an increase of relative humidity, and sulfate dominated when the air mass back trajectories passed through the Los Angeles port region. Understanding BBA aging processes and quantifying the size-resolved mass and number concentrations are important in determining the overall impact of wildfires on air quality, health, and climate.

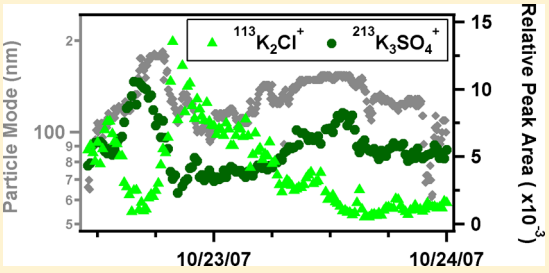

1. INTRODUCTION

Biomass burning leads to substantial atmospheric emissions of trace gases and a high number of mass concentrations of biomass burning aerosols (BBAs), which significantly impact climate and air quality.[1−3] BBAs perturb climate by scattering and absorbing solar radiation and by serving as cloud condensation nuclei.[2,3] BBAs have also been associated with adverse health impacts, including during the 2003 southern California wildfires when higher $PM_{2.5}$ concentrations were correlated to increased emergency room visits for respiratory problems.[4,5] Understanding how different chemical species are partitioned between individual BBA particles is critical to developing an understanding of the full range of environmental impacts of BBAs.[6−9] However, the majority of previous biomass burning studies have focused on bulk BBA properties with an emphasis on mass, which has limited our overall understanding of their evolution in the atmosphere and ultimate impacts on health and climate.[3]

The composition of BBAs depends strongly on fire type. Hotter, flaming fires produce particles containing higher fractions of inorganic material, such as potassium (K) along with increased soot content, while lower temperature smoldering fires emit more organic carbon-rich aerosols.[3,10] The physicochemical properties of freshly emitted BBAs change rapidly due to changing flame conditions, interactions with gas-phase species within the biomass burning plume, and interactions with other regional pollutants. Furthermore, photochemical reactions, cloud processing, and coagulation are important pathways in transforming BBAs. All of these processes cause the count median diameter (CMD) of fresh BBAs to grow from ∼100−160 nm to ∼120−230 nm.[3] Fresh BBAs typically contain potassium chloride (KCl) salts, which can heterogeneously react with secondary acids, such as nitric acid ($HNO_{3(g)}$) and sulfuric acid ($H_2SO_{4(g)}$);[11,12] thus, as BBAs age, KCl is replaced with potassium nitrate (KNO_3) and potassium sulfate (K_2SO_4). Both K and levoglucosan, which is emitted from the thermal breakdown of cellulose, are established tracers for BBA.[11−14] However, recent studies have determined that levoglucosan concentrations produced during biomass burning depend on fuel and fire conditions[15−17] and have shown that levoglucosan decomposes through photooxidation, exposure to the hydroxyl radical, and oligomerization.[18−20] Although smoke particles are typically large enough to be good CCNs regardless of their composition, the ratio of inorganic to water-soluble organic carbon species, such as

Received: January 27, 2013
Revised: May 30, 2013
Accepted: June 10, 2013
Published: June 10, 2013

 © 2013 American Chemical Society dx.doi.org/10.1021/es4004137 | Environ. Sci. Technol. 2013, 47, 7633−7643

levoglucosan and oxalic acid, is important for particle hygroscopicity.[6,9] Therefore, more information is needed on the composition of both freshly emitted BBAs as well as the extent of processing of different BBA particle types.

For the past few decades, the frequency of wildfires and land area burned has increased in the western U.S. due to regional warming, earlier spring arrival, and increased droughts.[21] The October 2007 wildfires, which burned >360 000 acres in San Diego County, were propagated by the rapid and dry easterly Santa Ana winds. These wildfires provided a unique opportunity to investigate their impact on regional air quality and to directly analyze the mixing state and evolution of BBAs over time. Measurements herein are the first observations of BBAs aging from ground-based single-particle measurements during intense local wildfires. Through positive matrix factorization (PMF) and single particle analysis, BBA chemical markers were probed in order to try to identify how different species were formed. To our knowledge, this is the first study that uses positive matrix factorization analysis to investigate the chemical evolution of single particles from a specific source.

2. EXPERIMENTAL SECTION

Ambient aerosol sampling was conducted at Urey Hall (32°52′31.66″ N, 117°14′28.64″ W) at the University of California, San Diego (UCSD) from 10/22/2007 12:00 to 11/1/2007 12:00 (Figure S1). Given the opportunistic nature of this study, measurements commenced one day after the Witch Fire began (10/21/2007 11:00). During the first week of the fires, the public was urged to stay home, and most public institutions and private businesses were closed.[22] Therefore, the contribution of aerosols from mobile sources was primarily limited to emergency vehicles during this time.

2.1. Peripheral Instrumentation. Size distributions of 10−590 nm and 0.6−20 μm particles were measured continuously and averaged every 5 min with a scanning mobility particle sizer (SMPS, TSI 3936) and averaged every minute with an aerodynamic particle sizer (APS, TSI 3321) at UCSD. Hourly concentrations of $PM_{2.5}$ mass were obtained from the California Air Resources Board (CARB, http://www.arb.ca.gov/aqmis2/aqdselect.php) for the Escondido and downtown San Diego sites. Although plume dynamics can lead to large gradients in concentration, a comparison between these sites and the measuring location is nonetheless useful. The SMPS and APS size resolved particle concentrations measured at UCSD were transformed into $PM_{2.5}$, $PM_{1.0}$, and $PM_{0.12-0.4}$ mass concentrations, assuming spherical particles with a density of 1.2 g/cm^3, appropriate for BBAs.[3] Meteorological data were obtained from the California Irrigation Management Information System (CIMIS) at three different sites: Escondido, downtown San Diego, and Torrey Pines. Figure S1 identifies all the sampling sites and the wildfire perimeters. The Escondido, downtown San Diego, and Torrey Pines sites are ∼30, 20, and 3 km away from UCSD, respectively.

2.2. ATOFMS Instrument and Data Analysis. Individual particle size and composition measurements were obtained in real-time with an ultrafine aerosol time-of-flight mass spectrometer (ATOFMS), without the MOUDI precut to allow measurement of particle sizes over a broader range, 120−1000 nm.[23] Briefly, particles enter the ATOFMS through an aerodynamic focusing lens and are accelerated to their size-dependent terminal velocities before traversing two 532 nm continuous wave lasers beams 6 cm apart. The calculated particle velocity is used to time the firing of a Q-switched 266 nm Nd:YAG laser, which desorbs and ionizes the chemical constituents of each particle. The generated positive and negative ions are detected using a dual polarity reflectron time-of-flight mass spectrometer.

Although 120−1000 nm particles were sampled with the ATOFMS, only 120−400 nm particles were analyzed herein, as this was the size range where the majority of BBAs were observed. Mass spectra were obtained for a total of 900 143 particles in the 120−400 nm aerodynamic diameter size range. These mass spectra were analyzed in the YAADA (www.yaada.org) toolkit for Matlab and were subsequently clustered with the neural network algorithm ART-2a, which separates the main particle types into clusters based on their unique ion patterns.[24] The particle clusters were named based on the most intense ion peaks and do not reflect all of the chemical species present. Clusters of similar ion patterns of varying intensities were manually combined, resulting in a total of four major classes: BBAs,[25,26] ocean-faring ships combusting heavy fuel oil (HFO),[27,28] organic carbon (OC),[29,30] and soot.[30,31] The remaining particle types made up <2% of particle number and were thus combined into the "other" category.

The identified peaks at each m/z provide the most likely assignment based on previous lab and field studies. Relative peak areas (RPAs), defined as the normalized peak area of one ion to the total ion intensity, minimize the variability in peak intensity compared to absolute peak areas in particles of the same matrix.[32] The average RPAs of 120−400 nm BBAs were determined for 19 markers previously observed in ATOFMS studies:[25,29,33−38] sulfate ($^{97}HSO_4^-$), nitrate ($^{62}NO_3^-$), nitrite ($^{46}NO_2^-$), nitric acid ($^{125}HNO_3NO_3^-$), ammonium ($^{18}NH_4^+$), oxalate ($^{89}HC_2O_4^-$), potassium chloride ($^{113}K_2Cl^+$), potassium nitrate ($^{140}K_2NO_3^+$), potassium sulfate ($^{213}K_3SO_4^+$), organic carbon markers ($^{27}C_2H_3^+$, $^{43}C_2H_3O^+$, $^{59}CH_3CO_2^-$, $^{71}C_3H_3O_2^-$, $^{73}C_2HO_3$/ $C_3H_5O_2^-$, $^{75}C_2H_3O_3^-$, and $^{87}C_3H_3O_3^-$), organic nitrogen fragments ($^{26}CN^-$ and $^{42}CNO^-$), and an amine marker ($^{86}(C_2H_5)_2NCH_2^+$). Average RPAs for each of these species were determined every 15 min as well as by particle size every 10 nm. Due to ambiguity and interference, several markers could not be used in this study. The strong $^{39}K^+$ signal on BBAs often causes distinct cross talk interference in the negative mass spectra between −33 to −38 m/z. Thus, due to the prevalence of this cross talk, the chloride ions ($^{35,37}Cl^-$) were not utilized in this study. In addition, due to significant interference of a broad $^{46}NO_2^-$ ion peak, the formate ion ($^{45}HCO_2^-$) was not analyzed either.

2.3. Positive Matrix Factorization Analysis. In order to complement single particle data analysis, positive matrix factorization (PMF) was performed using BBA chemical markers. PMF, which implicitly assumes that temporally covarying species have the same origin, is a multivariate receptor model used to determine source factors.[39−41] PMF has been used extensively with aerosol data, typically with speciated mass concentrations. However, particle types based on mass spectra have also been analyzed with PMF previously to elucidate source emissions, chemical processing, and transport of particles.[42−45] In contrast, this current study used PMF exclusively to analyze the chemical aging of the BBA mixing state and, to our knowledge, is the first use of PMF to study the chemical evolution of individual ambient particles from the same source. The Environmental Protection Agency's (USEPA) PMF 3.0 model[46] was used to generate source factors based on the 15 min averaged RPAs for the 19 primary

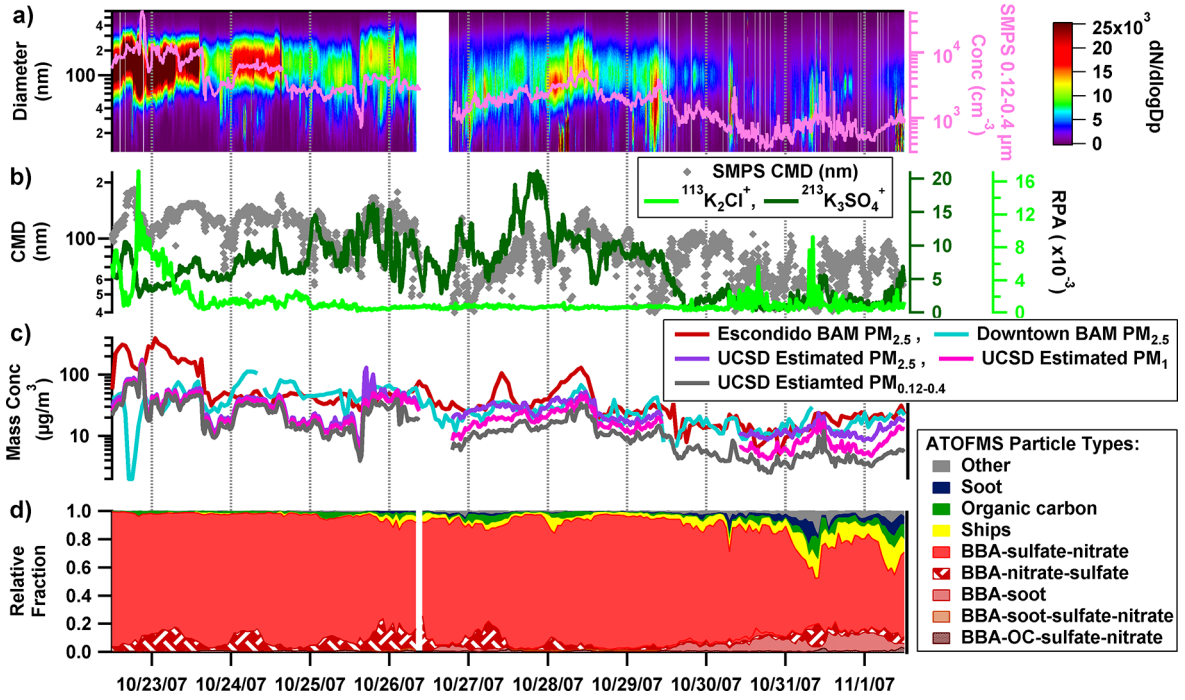

Figure 1. (a) 10−600 nm ambient particle size distribution from SMPS, (b) SMPS count median diameter with $^{113}K_2Cl^+$ and $^{213}K_3SO_4^+$, (c) mass concentrations, and (d) temporal distribution of 120−400 nm ambient particle types measured with the ATOFMS. White space indicates no data obtained in that time period.

and secondary BBA markers listed in section 2.2. These species were utilized because of their relevance in biomass burning and abundance during the 2007 San Diego wildfires. For this study, an uncertainty of 50% in RPA was used since the ATOFMS laser shot-to-shot fluctuations and particle matrix effects may affect the resulting individual mass spectral peaks significantly. PMF solutions with 3−13 factors were explored, and the 10-factor solution was chosen as the best because the measured versus predicted RPA of chemical species in the PMF model had strong correlations (R^2 = 0.85−0.99) while providing the most physically meaningful factors.[41,46] Further details considered during data preparation and PMF analysis are given in the Supporting Information.

3. RESULTS AND DISCUSSION

Figures S2 and S3 show the meteorological parameters during this study. Strong easterly Santa Ana winds, with high temperatures, low relative humidity (RH), and fast wind speeds, were observed during the first two days of the fires (10/21/2007 to 10/23/2007 16:00). These first two days showed almost no diurnal RH and temperature patterns, especially at Escondido. This period also exhibited the most intense wildfires, which were propagated by the Santa Ana winds toward the more populated western side of San Diego County, as shown by the satellite image in Figure S4. The air mass back trajectories modeled with HYSPLIT 4.0[47] (Figure S5) indicate that during the intense Santa Ana winds, UCSD was directly downwind of the Witch Fire, the largest fire during the study. On the basis of the average wind speed (7 m/s) during the first two days of sampling, the wildfire emissions took ∼70 min to travel from the Witch Fire around Escondido to the sampling site at UCSD.

After 10/23/2007 22:00, the air mass sampled originated further southeast compared to the previous two days, thus missing the dense wildfire emissions near Escondido (Figure S5). Figure 1 shows an abrupt reduction in the particle number concentrations measured at UCSD coincident with the sudden decrease in $PM_{2.5}$ at Escondido during the evening of 10/23/2007. After this shift, the RH and temperature profiles at Escondido regained their diurnal profile, while those at Torrey Pines and San Diego took a bit longer. The wildfire emissions flowed offshore until the afternoon of 10/25/2007 (Figure S4), when the wind shifted onshore, although remaining fairly stagnant. After this switch in air mass direction, the RH at Torrey Pines increased from <35% to >90%. Between 10/26/2007 10:00 and 10/28/2007 04:00, the air continued to flow from the Pacific Ocean but from further away from the coast. During this period there was a significant fog event on 10/27/2007, which limited the amount of solar radiation (Figure S3). Between 10/28/2007 10:00 and 10/29/2007 10:00, the air masses sampled passed above the Harris Fire, which burned along the border with Mexico. Toward the end of the study, between 10/29/2007 16:00 and 10/30/2007 22:00, the air mass sampled at UCSD passed close to the Ports of Los Angeles and Long Beach, bringing aged BBAs onshore possibly mixed with ocean-going ship and port emissions. Finally, after 10/31/2007, the air originated inland through Riverside, California.

3.1. Particle Number and Mass Concentrations. Figure 1a shows the SMPS size distribution as a function of time. The highest particle concentrations were between 50 and 400 nm during the most intense wildfire period (10/22/2007 to 10/23/2007), thereby confirming this was the period when UCSD received the most wildfire emissions. Specifically, there was a spike in SMPS 120−400 nm particle number concentrations at 10/22/2007 20:00−22:00 going from ∼10 000 to ∼40 000 cm^{-3} and back to ∼10 000 cm^{-3}. Additionally, the CMD of the particles shifted rapidly on 10/22/2007 to 10/23/2007 (Figure 1b) increasing from ∼100 to ∼170 nm between 10:00 and 18:00 on 10/22/2007, and decreasing back to ∼100 nm by 10/

dx.doi.org/10.1021/es4004137 | Environ. Sci. Technol. 2013, 47, 7633−7643

22/2007 23:00. The CMD increased again from 10/22/2007 23:00 to 10/23/2007 9:00, at which time the CMD remained stable at ∼140 nm. The CMD decreased to ∼100 nm on the morning of 10/25/2007 and then increased to ∼180 nm coinciding with the increase of RH on the afternoon of 10/25/2007. After 10/27/2007, the effects of the wildfires were less evident on the particle size distributions, and periodically an ultrafine mode, indicative of local traffic emissions, was observed. The observed particle CMD of 100−180 nm at the beginning of this study are comparable to the range of previously measured BBAs between 100 and 230 nm depending on particle age.[3,48,49] The broad CMD range observed indicates BBAs were processed to different degrees during transport from the wildfires to the UCSD sampling site or alternatively that fire conditions changed.[50] Detailed analysis linking chemical markers of fresh and aged BBAs with the shifts in size distribution are described in section 3.3.

Figure 1c shows the $PM_{2.5}$ measured at Escondido and downtown San Diego along with the estimated mass concentrations at UCSD. Due to the proximity of the Witch and Poomacha Fires (Figure S1), the $PM_{2.5}$ concentrations were higher at Escondido than at UCSD and downtown. However, the national ambient air quality air standard (NAAQS) 24-h average $PM_{2.5}$ exposure limit of 35 $\mu g/m^3$ was exceeded at all sites, with hourly maximum values as high as 397, 177, and 110 $\mu g/m^3$ at Escondido, UCSD, and downtown, respectively. During 10/22/2007 12:00 to 10/23/2007 16:00, when the wildfires were most intense and air mass trajectories passed through the Witch Fire before arriving at UCSD, the $PM_{2.5}$ concentrations were highest with median (interquartile range) values of 72.0 (43.0−186.0), 47.6 (35.1−61.7), and 42.0 (29.5−48.3) $\mu g/m^3$ at Escondido, UCSD, and downtown, respectively. In contrast, the annual 2007 average ± standard deviation $PM_{2.5}$ concentrations were 15.0 ± 17.5 and 10.9 ± 9.1 $\mu g/m^3$ at the Escondido and downtown air quality stations, respectively. Therefore, the 2007 wildfires emitted high fine aerosol mass concentrations dangerous to the public health of communities downwind. Estimated $PM_{1.0}$ and $PM_{0.1-0.4}$ from particle size concentrations at UCSD were also the highest throughout the period of intense wildfires (10/22/2007 12:00 to 10/23/2007 16:00) with median (interquartile range) values of 44.5 (30.9−56.3) and 37.7 (26.6−48.5) $\mu g/m^3$ and maximum values of 168 and 148 $\mu g/m^3$, respectively. The majority of particle mass was due to particles <400 nm. For example, during the period of intense wildfires, total $PM_{0.1-0.4}$ mass concentrations contributed to 81.2% of the $PM_{2.5}$ and 87.5% of $PM_{1.0}$ at UCSD. This is contrary to normal ambient aerosols in which larger particles contribute the majority of particle mass, an important observation since particle size plays a role in adverse health effects.[51−53]

Muhle et al. estimated $PM_{2.5}$ concentrations at UCSD during the 2003 wildfires as high as 250 $\mu g/m^3$, higher concentrations than those estimated during the 2007 wildfires.[48] The higher $PM_{2.5}$ concentrations in 2003 were due to different fire and meteorological conditions, in addition to fire proximity. A previous study at UCSD's Scripps Institution of Oceanography (SIO) during a Santa Ana event determined that the 30-min-averaged $PM_{2.5}$ was only 7 $\mu g/m^3$,[54] indicating that the high mass concentrations observed during the 2003 and 2007 wildfires were not caused by the Santa Ana winds alone, but rather by the wildfires themselves. In contrast, the estimated $PM_{1.0}$ at the SIO pier was as high as 30 $\mu g/m^3$ during a previous period of pollution transport from the ports of Los Angeles.[55] Therefore, large wildfires, with maximum $PM_{1.0}$ concentrations of 177 and 250 $\mu g/m^3$ during the 2007 and 2003 wildfires, can contribute >5 times higher submicrometer aerosol mass concentrations than regional pollution transport events in San Diego.

3.2. Particle Types. Figure 1d shows the temporal variation of particle types between 120 and 400 nm. After 10/30/2007, the relative amounts OC and soot increased. The ocean-faring ship particle type became more prevalent after 10/31/2007. Although all BBA mass spectra have similar characteristics, including $^{39}K^+$ and carbonaceous markers,[25] five different BBA particle types were observed in this study (Figure S6) based on the relative strength of the carbonaceous markers, $^{62}NO_3^-$, and $^{97}HSO_4^-$. Combined together, the BBA particle types represented ∼84% of the total number of particles detected by the ATOFMS, although nearly 100% of all particles were BBAs until 10/25/2007.

It should be noted that BBA particles were sampled after transport to UCSD, and thus the particles had undergone various degrees of aging. The known marker of fresh BBAs,[10,12,57] $^{113}K_2Cl^+$, peaked on 10/22/2007 when particles with the smallest SMPS CMD (∼100 nm) were detected, confirming the presence of fresh BBAs (Figure 1b). However, when the SMPS CMD increased to ∼170 nm, also on 10/22/2007, the peak area of $^{113}K_2Cl^+$ decreased while that of $^{213}K_3SO_4^+$ increased, and thus these chemical markers serve as effective indicators of the relative physical age of BBAs. These changes in BBA size and composition with age will affect particle hygroscopicity and the overall cloud nucleating properties of BBAs and hence play an important role in regional climate.[56]

In this study, 44−65% of BBA mass spectra had peaks at $^{71}C_3H_3O_2^-$, $^{73}C_2HO_3^-/C_3H_5O_2^-$, $^{75}C_2H_3O_3^-$, and $^{87}C_3H_3O_3^-$ likely due to organic acid anions, which typically produce negative molecular ions, such as oxalate ($^{89}HC_2O_4^-$).[36] Although Silva et al.[25] concluded that $^{45}HCO_2^-$, $^{59}CH_3COO^-$, and $^{71}C_3H_3O_2^-$ were indicative of levoglucosan, other ATOFMS studies with organic standards, meat burning, and plant detritus showed that these ions were not unique to levoglucosan.[29,57] As explained in section 2.2, $^{45}HCO_2^-$ was not used in this study due to interference. Because levoglucosan is primarily emitted from biomass burning, it should be found across all BBA sizes. However, because the size distribution of BBA with $^{71}C_3H_3O_2^-$ was shifted toward particles >225 nm (Figure S7), $^{71}C_3H_3O_2^-$ must be mostly secondary in this study. Similar results were found for $^{59}CH_3COO^-$.These results suggest that $^{59}CH_3COO^-$ and $^{71}C_3H_3O_2^-$ observed in BBA during this study were not representative of levoglucosan. In order to try to identify the $^{71}C_3H_3O_2^-$, $^{73}C_2HO_3^-/C_3H_5O_2^-$, $^{75}C_2H_3O_3^-$, and $^{87}C_3H_3O_3^-$ ions, organic standards were analyzed with ATOFMS. Figure S8 shows representative mass spectra of acrylate, glyoxalate, and other standards, in addition to levoglucosan, highlighting that multiple compounds typically present in biomass burning emissions can produce these ions. Thus, it is not possible to identify the source of these ions using solely the ATOFMS. However, the prevalence of these ions on larger particles suggests that these peaks resulted from the condensation of secondary organic acids. More information on how these standards were analyzed and a discussion of these results are given in the Supporting Information.

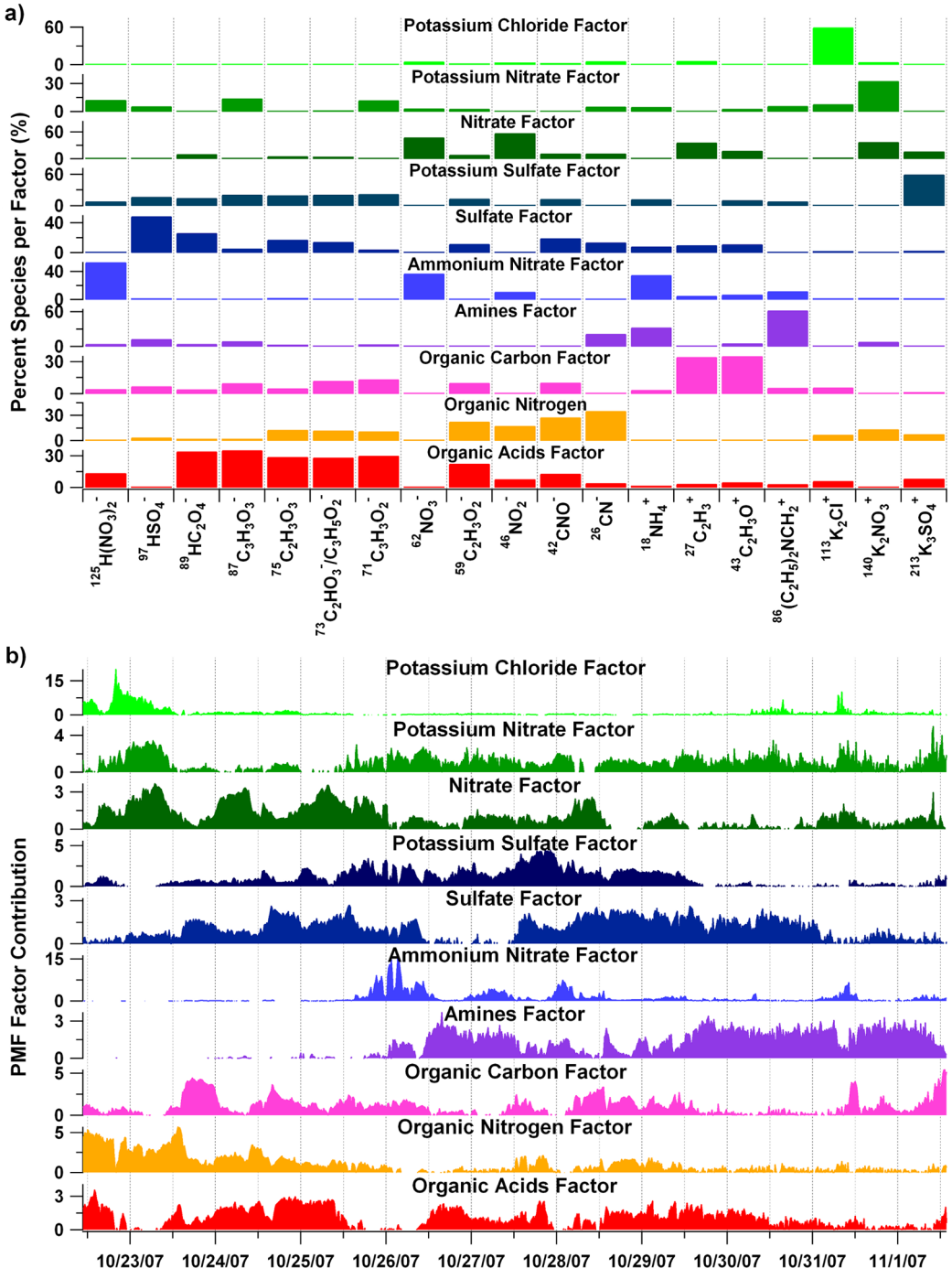

Figure 2. The PMF results with 10 factors: (a) the source profiles, where each profile was named based on the most abundant species, and (b) temporal distribution of each factor.

3.3. PMF Factors and Single Particle Analysis. The 10-factor PMF profiles and temporal distribution for 120−400 nm BBAs are shown in Figure 2 and described in the following sections. The PMF factors were named based on the most abundant species present and are presented in italics. All species were separated into multiple factors; each factor may have a unique formation mechanism based on meteorology and/or environmental conditions. The size and temporal profiles of representative RPAs for each PMF factor are shown in Figure 3. The different fuels and fire conditions at each of the five wildfires could have also contributed to differences in the BBA composition measured. Finally, it is worth noting that the following discussion related to particle aging is qualitative due to the distance of the wildfires from the sampling site, the shifts in wind direction, and the differences in microclimate as the air mass traveled.

3.3.1. Inorganic Species. The *potassium chloride factor, potassium nitrate factor, and potassium sulfate factor* were mainly associated with $^{113}K_2Cl^+$, $^{140}K_2NO_3^+$, and $^{213}K_3SO_4^+$, respectively, as shown in Figure 2a. The *potassium chloride factor*, which peaked on 10/22/2007 (Figure 2b), was assigned as the freshest BBA sampled. $^{140}K_2NO_3^+$ and $^{213}K_3SO_4^+$, which are

dx.doi.org/10.1021/es4004137 | Environ. Sci. Technol. 2013, 47, 7633−7643

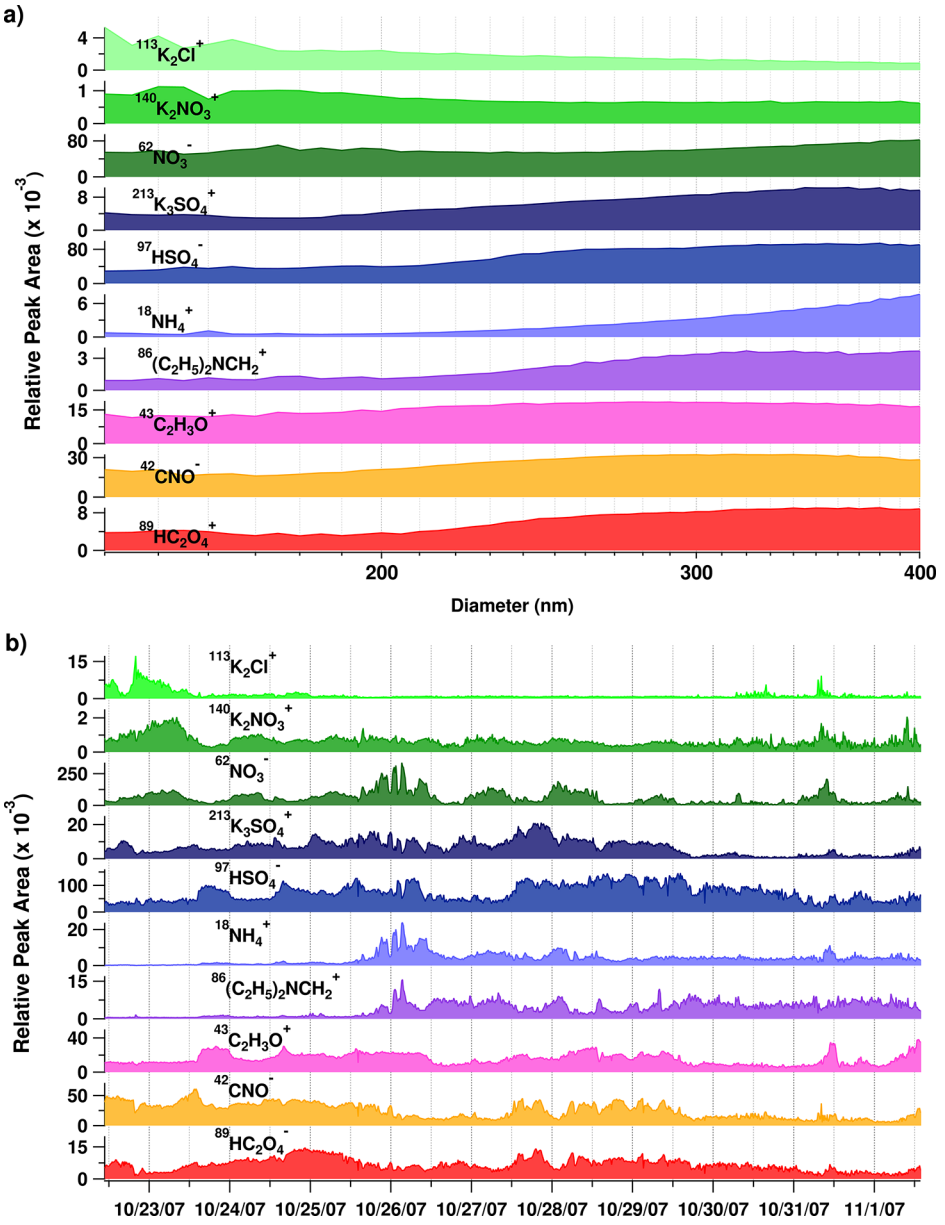

Figure 3. (a) Size and (b) temporal distribution of the BBA relative peak areas most representative of each factor.

indicative of more aged BBA, peaked at different times than $^{113}K_2Cl^+$ (Figure 3a). Following the decline of $^{113}K_2Cl^+$, there was a steady increase of $^{140}K_2NO_3^+$ on 10/22/2007 until it peaked on the morning of 10/23/2007, indicating that the majority of KCl was first transformed to KNO_3 through heterogeneous reactions with $HNO_{3(g)}$. $^{213}K_3SO_4^+$ peaked between 10/25/2007 and 10/30/2007, indicating that potassium salts in BBA were further transformed to K_2SO_4 by reaction with $H_2SO_{4(g)}$. The continuous high temporal resolution of data every 15 min for 10 days indicating BBA potassium salts underwent heterogeneous reactions in this study is unprecedented. Moreover, particles grow in size temporally as they coagulate or as secondary species condense onto them. A comparison of the size distribution of particles containing $^{113}K_2Cl^+$, $^{140}K_2NO_3^+$, and $^{213}K_3SO_4^+$ (Figure 3a) highlights that the smaller and hence fresher particles are those with KCl and KNO_3 (with modes at 140 and 155 nm, respectively) compared to the larger and hence more aged particles with K_2SO_4 (with mode at 360 nm). Fresh (*potassium chloride factor*), slightly aged (*potassium nitrate factor*), and moderately aged (*potassium sulfate factor*) plumes from the San Diego wildfires were sampled during this study, as characterized by the temporal and size distribution of potassium salts in BBAs. Figure 3a shows that the size distributions of the nonpotassium salt markers, with the exception of $^{62}NO_3^-$ and $^{43}C_2H_3O^+$, were larger than those of $K_3SO_4^+$. These larger and hence more aged BBAs were characterized by the lack of potassium salts and the presence of secondary species such as $^{97}HSO_4^-$, $^{18}NH_4^+$, $^{86}(C_2H_5)_2NCH_2^+$, and $^{89}HC_2O_4^-$. It is likely that these aged BBAs still contained potassium salts, but that they were coated with significant amounts of secondary species, masking their presence when analyzed with the ATOFMS.[58] Thus, in addition to the fresh, slightly aged, and moderately aged BBAs, aged BBAs were also sampled in this study.

Although particulate phase nitrate and sulfate are typically secondary species, they can be primarily emitted during biomass burning. Because $^{62}NO_3^-$ was found fairly uniformly across all sizes whereas $^{97}HSO_4^-$ was found predominantly in

dx.doi.org/10.1021/es4004137 | Environ. Sci. Technol. 2013, 47, 7633−7643

BBAs > 225 nm (Figure 3a), it can be concluded that $^{62}NO_3^-$ was present in all stages of aging, while $^{97}HSO_4^-$ was only found in aged BBAs. This conclusion is supported by a previous aircraft study of BBAs over Wyoming, which also determined that aged BBAs contained more $^{97}HSO_4^-$ compared with $^{62}NO_3^-$.[9] In contrast, a previous Mexico City study observed more $^{62}NO_3^-$ than $^{97}HSO_4^-$ in aged BBAs.[33] The difference in the abundance of HSO_4^- versus $^{62}NO_3^-$ in aged BBAs is likely dependent on the concentrations of different precursor gas phase species and meteorological conditions. For example, high humidity and increased cloud cover were likely more abundant in the air mass during the aircraft BBA study in order for extensive cloud processing of BBAs to occur, whereas in the Mexico City study there were probably higher concentrations of $NO_{x(g)}$ and solar radiation, leading to increased photochemistry.

Overall, the *nitrate factor* and *sulfate factor* followed the temporal variations of $^{62}NO_3^-$ and $^{97}HSO_4^-$, respectively (Figure 2b). BBA $^{62}NO_3^-$ exhibited a diurnal pattern at the beginning of the fires, reaching a maximum in the midmorning and decreasing at noon when the temperature was the highest. Thus, the likely mechanism involved in this diurnal pattern is partly explained by the semivolatile nature of the nitrate, which makes the ambient temperature an important driver for its partitioning between the gas and particulate phases. The NO_x temporal distribution (Figure S9) was characterized with a maximum during the midmorning and a smaller one at night. Thus, in addition to temperature, photochemistry must be playing a role. Despite the thick haze over San Diego County during the wildfires, solar radiation still had a strong diurnal profile overall (Figure S3), and thus photochemistry probably initiated the rapid conversion of $NO_{x(g)}$, emitted directly from the wildfires, to $HNO_{3(g)}$, which would then partition to the particulate phase as nitrate.[59] The addition of nitrate to BBA is representative of BBA aging due to interaction with wildfire coemissions in the presence of the appropriate meteorological conditions.

When the RH increased on 10/25/2007 (Figure S3), the *nitrate factor* no longer tracked $^{62}NO_3^-$, which spiked in parallel with $^{125}HNO_3NO_3^-$ and $^{18}NH_4^+$ during this period (Figure 3b). Instead, PMF analysis separated this $^{62}NO_3^-$ spike into the *ammonium nitrate factor*. The high humidity probably led to the formation of particulate phase NH_4NO_3 from gaseous NH_3 and HNO_3,[60,61] both of which are emitted from biomass burning.[62−66] Albeit the $^{18}NH_4^+$ was associated with $^{97}HSO_4^-$ during the rest of the study, indicating the presence of ammonium sulfate ($(NH_4)_2SO_4$), when the *ammonium nitrate factor* spiked there was a prevalence of ammonium nitrate (NH_4NO_3; Figure S10), as previously observed in BBAs.[59,67] It is worth noting that sulfate was found in smaller particle sizes than those with ammonium (Figure 3a) and that ammonium was often mixed with nitrate in the larger sized particles. Although previous BBA studies have also found correlations between ammonium and oxalate,[68] in the current study these species were independent of each other.

Though present at the beginning of the fires, the RPA of $^{97}HSO_4^-$ remained low until the afternoon of 10/23/2007 and then peaked mostly in the afternoons between 10/23/2007 and 10/26/2007 (Figure 3b). Although in-cloud aqueous processing of $SO_{2(g)}$ is the main formation pathway of sulfate,[69,70] the RH remained low (<40%), even at night, until 10/25/2007 due to the Santa Ana winds, limiting the aqueous conversion of $SO_{2(g)}$ to sulfate. Thus, the $^{97}HSO_4^-$ peaks on 10/23/2007 and 10/24/2007 may be a result of primary sulfate emissions from the wildfires. Once the Santa Ana winds dissipated on 10/25/2007, the air mass sampled originated over the oceans instead of over land (Figure S5), consistent with the presence of the ship particle type (Figure 1d). Although the RH increased to >90% during this change, $^{97}HSO_4^-$ did not increase in parallel to the RH likely because of low SO_2 atmospheric concentrations. Additionally, because shipping is a more significant source of $SO_{2(g)}$ than biomass burning,[71] the $^{97}HSO_4^-$ detected on BBA after 10/25/2007 likely originated from $SO_{2(g)}$ emitted from the ships around the ports of San Diego, Los Angeles, and Long Beach, facilitating the formation of sulfate through cloud processing, perhaps over the ocean, during this time. The 10/27/2007 $^{97}HSO_4^-$ spike coincided with the presence of a widespread fog event, indicating it was produced through aqueous processing during this time. Therefore, the addition of sulfate to BBA at the end of this study is representative of BBA aging upon interaction with regional pollutants depending on meteorology. BBAs in areas affected by different regional pollutants and meteorological conditions will exhibit different aging processes.

3.3.2. Organic Carbon Species. As illustrated in Figure 2, PMF analysis separated organic carbon markers into four distinct factors described below with species given in order of prevalence. The *organic carbon factor* was mainly composed of $^{43}C_2H_3O^+$ and $^{27}C_2H_3^+$, which are organic carbon fragments resulting from the ionization of larger organic carbon species. The *organic carbon factor* tracked the temporal profile of the *sulfate factor* while the RH remained low on the afternoons of 10/23/2007 and 10/24/2007 (Figure 2b), suggesting that the organic species represented by the $^{43}C_2H_3O^+$ and $^{27}C_2H_3^+$ fragments were formed through a similar primary mechanism as sulfate during this time.

The *organic nitrogen factor*, comprised of $^{26}CN^-$, $^{42}CNO^-$, $^{59}C_2H_3O_2^-$, and $^{46}NO_2^-$, was more prevalent at the beginning of the wildfires. The $^{26}CN^-$ and $^{42}CNO^-$ markers, which can be the resulting fragment of many nitrogen containing organic nitrogen species, have been observed in biogenic particles such as plant detritus and bacteria.[29,57,72] Heterocyclic nitrogen compounds, including some naturally produced by plants and living organisms, and water-soluble organic nitrogen species have been previously measured in BBAs.[73−75] Previous work has also observed significant gas phase hydrogen cyanide (HCN) and isocyanic acid (HCNO) emitted in fresh biomass burning;[76−79] however, based on the vapor pressure of these species they will not partition to the particulate phase. Thus, it is likely that the $^{26}CN^-$ and $^{42}CNO^-$ markers are resulting fragments of organic nitrogen biogenic material involved in biomass pyrolysis. Furthermore, rapid formation of gas phase acetic acid, seen as $^{59}C_2H_3O_2^-$, and other organic acids have been observed in relatively young biomass burning plumes.[15,79−81] Thus, it is likely that the species found in the *organic nitrogen factor* were either emitted directly in the particulate phase or they were rapidly produced from gas phase precursors emitted during flaming conditions and partitioned quickly to the particulate phase as the smoke plume cooled during transport.

The *amines factor* consisted mainly of $^{86}(C_2H_5)_2NCH_2^+$ with minor contributions from $^{18}NH_4^+$ and $^{26}CN^-$, which were both likely also amine fragments during this time. The *ammonium nitrate factor* spike, which coincided with the first increase in RH on the night of 10/25/2007 (Figure S3), was 12 h before

the *amines factor* grew in (Figure 2b). BBAs with $^{18}NH_4^+$ were also larger than those with $^{86}(C_2H_5)_2NCH_2^+$ (Figure 3a), likely because water drives nitrate onto the particulate phase as NH_4NO_3. The BBAs with $^{86}(C_2H_5)_2NCH_2^+$ also grew in size over time but did not grow as large as the BBAs with $^{18}NH_4^+$ (Figure 3a). It is also interesting that the *amines and organic nitrogen factors* were split into two, but based on their temporal and size profiles this makes sense. While the *organic nitrogen factor* was prevalent at the beginning of the fires, the *amines factor* spiked after the increase in RH on 10/25/2007. In controlled laboratory burns, gas-phase amines have been observed to be emitted during the smoldering phase.[1,62] Amines remained in the gas phase while the RH was low, as shown by previous work,[38,82] and partitioned to the particulate phase once the RH increased to >90%.

The *organic acids factor*, which had contributions from $^{89}HC_2O_4^-$, $^{87}C_3H_3O_3^-$, $^{75}C_2H_3O_3^-$, $^{73}C_2HO_3^-/^{73}C_3H_5O_2^-$, and $^{71}C_3H_3O_2^-$, peaked between 10/22/2007 12:00 and 10/22/2007 19:00, 10/23/2007 9:00 and 10/25/2007 14:00, 10/26/2007 10:00 and 10/27/2007 22:00, and 10/28/2007 5:00 and 10/30/2007 11:30. These organic acids tracked each other temporally and by size (Figure S7), indicating similar formation mechanisms, which may have varied during the sampling period due to changing meteorological conditions and differing concentrations of gas-phase precursors. The organic acids at the beginning of the wildfires were likely primary or a result of fast secondary production, as has been previously observed.[15,80,81] However, organic acids spiked between 10/28/2007 5:00 and 10/30/2007 11:30, coinciding with the period when the air mass back trajectories came from offshore, and thus the BBAs sampled during this time had significantly more time to age. Therefore, the organic acids from this period could have formed through slow gas-to-particle conversion of VOCs emitted during biomass burning, which further oxidized into the organic acids.[83,84]

Although it was not possible to identify each organic species present in BBAs, the four different organic carbon factors identified in this study indicate that ATOFMS data can still be used to learn about different processes that occur in biomass burning. New methods for online sampling of BBA would be useful, such as the aerosol chip electrophoresis (ACE) system[85] and the two-dimensional gas chromatography thermal desorption (2D-TAG) instrument,[86] in order to complement the capabilities of ATOFMS measurements. In addition, it would be greatly beneficial to sample ultrafine (<100 nm) BBA with the combined growth tube ATOFMS approach[87] to investigate mixing state differences in individual particles smaller than can currently be sampled with the ATOFMS alone.

During the 2007 San Diego wildfires, BBAs were found to contribute significantly to high particulate mass concentrations with $PM_{0.12-0.4}$ as high as 148 $\mu g/m^3$. In addition, BBAs were observed undergoing various aging pathways based on changes in their particle size, mixing state, and PMF factors. Potassium chloride and organic nitrogen factors were dominant during the beginning of the wildfires, while ammonium nitrate and amines factors spiked after an increase of relative humidity, and sulfate was prevalent when the air mass back trajectories passed through the port region in Los Angeles before arriving at the sampling site. Finally, evidence of potassium salts heterogeneously reacting with inorganic acids was detected with continuous high temporal resolution for the first time.

■ ASSOCIATED CONTENT

Ⓢ Supporting Information

Map of the fires and sampling sites, meteorological data, backward air mass trajectories, satellite image, mass spectra, gas phase data, and ternary plots during the wildfires are shown in SI. This information is available free of charge via the Internet at http://pubs.acs.org.

■ AUTHOR INFORMATION

Corresponding Author

*Fax: 858-534-7042. E-mail: kprather@ucsd.edu.

Present Addresses

∥California Council on Science and Technology, Sacramento, CA

⊥Department of Civil Engineering, City College of New York, City University of New York, New York, NY

#Environ International Corporation, Groton, MA

▽Department of Atmospheric Sciences, University of Washington, Seattle, WA

Notes

The authors declare no competing financial interest.

■ ACKNOWLEDGMENTS

Dr. Andrew Ault, Joe Mayer, Dr. Ryan Sullivan, and Maggie Yandell are acknowledged for help collecting data and John Cahill for comments that greatly improved the manuscript. We are also grateful for data collected by the California Air Resources Board (CARB) and the California Irrigation Management Information System (CIMIS). Funding for this study was provided by CARB Grant # 04-336 and the U.S. Environmental Protection Agency PM Center Grant # R832415.

■ REFERENCES

(1) Andreae, M. O.; Merlet, P. Emission of trace gases and aerosols from biomass burning. *Global Biogeochem. Cycles* **2001**, *15* (4), 955–966.

(2) Crutzen, P. J.; Andreae, M. O. Biomass burning in the tropics - impact on atmospheric chemistry and biogeochemical cycles. *Science* **1990**, *250* (4988), 1669–1678.

(3) Reid, J. S.; Koppmann, R.; Eck, T. F.; Eleuterio, D. P. A review of biomass burning emissions part II: intensive physical properties of biomass burning particles. *Atmos. Chem. Phys.* **2005**, *5*, 799–825.

(4) Delfino, R. J.; Brummel, S.; Wu, J.; Stern, H.; Ostro, B.; Lipsett, M.; Winer, A.; Street, D. H.; Zhang, L.; Tjoa, T.; Gillen, D. L. The relationship of respiratory and cardiovascular hospital admissions to the southern California wildfires of 2003. *Occup. Environ. Med.* **2009**, *66* (3), 189–197.

(5) Viswanathan, S.; Eria, L.; Diunugala, N.; Johnson, J.; McClean, C. An analysis of effects of San Diego wildfire on ambient air quality. *J. Air Waste Manage. Assoc.* **2006**, *56* (1), 56–67.

(6) Furukawa, T.; Takahashi, Y. Oxalate metal complexes in aerosol particles: implications for the hygroscopicity of oxalate-containing particles. *Atmos. Chem. Phys.* **2011**, *11* (9), 4289–4301.

(7) Jacobson, M. Z. Strong radiative heating due to the mixing state of black carbon in atmospheric aerosols. *Nature* **2001**, *409* (6821), 695–697.

(8) Zhou, Y. M.; Zhong, C. Y.; Kennedy, I. M.; Leppert, V. J.; Pinkerton, K. E. Oxidative stress and NF kappa B activation in the lungs of rats: a synergistic interaction between soot and iron particles. *Toxicol. Appl. Pharmacol.* **2003**, *190* (2), 157–169.

(9) Pratt, K. A.; Heymsfield, A. J.; Twohy, C. H.; Murphy, S. M.; DeMott, P. J.; Hudson, J. G.; Subramanian, R.; Wang, Z. E.; Seinfeld, J. H.; Prather, K. A. In Situ Chemical Characterization of Aged Biomass-

Burning Aerosols Impacting Cold Wave Clouds. *J. Atmos. Sci.* **2010**, *67* (8), 2451−2468.
(10) Posfai, M.; Simonics, R.; Li, J.; Hobbs, P. V.; Buseck, P. R. Individual aerosol particles from biomass burning in southern Africa: 1. Compositions and size distributions of carbonaceous particles. *J. Geophys. Res.* **2003**, *108* (D13), 8483 DOI: 10.1029/2002JD002291.
(11) Gaudichet, A.; Echalar, F.; Chatenet, B.; Quisefit, J. P.; Malingre, G.; Cachier, H.; Buatmenard, P.; Artaxo, P.; Maenhaut, W. Trace-Elements in Tropical African Savanna Biomass Burning Aerosols. *J. Atmos. Chem.* **1995**, *22* (1−2), 19−39.
(12) Li, J.; Posfai, M.; Hobbs, P. V.; Buseck, P. R. Individual aerosol particles from biomass burning in southern Africa: 2. Compositions and aging of inorganic particles. *J. Geophys. Res.* **2003**, *108* (D13), 8484 DOI: 10.1029/2002JD002310.
(13) Fraser, M. P.; Lakshmanan, K. Using levoglucosan as a molecular marker for the long-range transport of biomass combustion aerosols. *Environ. Sci. Technol.* **2000**, *34* (21), 4560−4564.
(14) Simoneit, B. R. T.; Schauer, J. J.; Nolte, C. G.; Oros, D. R.; Elias, V. O.; Fraser, M. P.; Rogge, W. F.; Cass, G. R. Levoglucosan, a tracer for cellulose in biomass burning and atmospheric particles. *Atmos. Environ.* **1999**, *33* (2), 173−182.
(15) Gao, S.; Hegg, D. A.; Hobbs, P. V.; Kirchstetter, T. W.; Magi, B. I.; Sadilek, M. Water-soluble organic components in aerosols associated with savanna fires in southern Africa: Identification, evolution, and distribution. *J. Geophys. Res.: Atmos.* **2003**, *108* (D13), 16.
(16) Sullivan, A. P.; Holden, A. S.; Patterson, L. A.; McMeeking, G. R.; Kreidenweis, S. M.; Malm, W. C.; Hao, W. M.; Wold, C. E.; Collett, J. L. A method for smoke marker measurements and its potential application for determining the contribution of biomass burning from wildfires and prescribed fires to ambient PM2.5 organic carbon. *J. Geophys. Res.* **2008**, *113* (D22302), DOI: 10.1029/2008JD010216.
(17) Harrison, R. M.; Beddows, D. C. S.; Hu, L.; Yin, J. Comparison of methods for evaluation of wood smoke and estimation of UK ambient concentrations. *Atmos. Chem. Phys.* **2012**, *12* (17), 8271−8283.
(18) Holmes, B. J.; Petrucci, G. A. Water-soluble oligomer formation from acid-catalyzed reactions of levoglucosan in proxies of atmospheric aqueous aerosols. *Environ. Sci. Technol.* **2006**, *40* (16), 4983−4989.
(19) Hennigan, C. J.; Miracolo, M. A.; Engelhart, G. J.; May, A. A.; Presto, A. A.; Lee, T.; Sullivan, A. P.; McMeeking, G. R.; Coe, H.; Wold, C. E.; Hao, W. M.; Gilman, J. B.; Kuster, W. C.; de Gouw, J.; Schichtel, B. A.; Collett, J. L., Jr.; Kreidenweis, S. M.; Robinson, A. L. Chemical and physical transformations of organic aerosol from the photo-oxidation of open biomass burning emissions in an environmental chamber. *Atmos. Chem. Phys.* **2011**, *11* (15), 7669−7686.
(20) Hennigan, C. J.; Sullivan, A. P.; Collett, J. L.; Robinson, A. L. Levoglucosan stability in biomass burning particles exposed to hydroxyl radicals. *Geophys. Res. Lett.* **2010**, *37*, 4.
(21) Westerling, A. L.; Hidalgo, H. G.; Cayan, D. R.; Swetnam, T. W. Warming and earlier spring increase western US forest wildfire activity. *Science* **2006**, *313* (5789), 940−943.
(22) *San Diego County Firestorms After Action Report*; EG&G Technical Services, Inc.: San Francisco, CA, 2007.
(23) Su, Y. X.; Sipin, M. F.; Furutani, H. F.; Prather, K. A. Development and characterization of an aerosol time-of-flight mass spectrometer with increased detection efficiency. *Anal. Chem.* **2004**, *76*, 712−719.
(24) Song, X. H.; Hopke, P. K.; Fergenson, D. P.; Prather, K. A. Classification of single particles analyzed by ATOFMS using an artificial neural network, ART-2A. *Anal. Chem.* **1999**, *71* (4), 860−865.
(25) Silva, P. J.; Liu, D.; Noble, C. A.; Prather, K. A. Size and Chemical Characterization of Individual Particles Resulting from Biomass Burning of Local Southern California Species. *Environ. Sci. Technol.* **1999**, *33* (18), 3068−3076.
(26) Guazzotti, S. A.; Suess, D. T.; Coffee, K. R.; Quinn, P. K.; Bates, T. S.; Wisthaler, A.; Hansel, A.; Ball, W. P.; Dickerson, R. R.; Neususess, C.; Crutzen, P. J.; Prather, K. A. Characterization of carbonaceous aerosols outflow from India and Arabia: Biomass/biofuel burning and fossil fuel combustion. *J. Geophys. Res.* **2003**, *108* (D15), 4485 DOI: 10.1029/2002JD003277.
(27) Ault, A. P.; Gaston, C.; Wang, Y.; Dominguez, G.; Thiemens, M. H.; Prather, K. A. Characterization of the Single Particle Mixing State of Individual Ship Plume Events Measured at the Port of Los Angeles. *Environ. Sci. Technol.* **2010**, *44* (6), 1954−1961.
(28) Healy, R. M.; O'Connor, I. P.; Hellebust, S.; Allanic, A.; Sodeau, J. R.; Wenger, J. C. Characterisation of single particles from in-port ship emissions. *Atmos. Environ.* **2009**, *43* (40), 6408−6414.
(29) Silva, P. J.; Prather, K. A. Interpretation of mass spectra from organic compounds in aerosol time-of-flight mass spectrometry. *Anal. Chem.* **2000**, *72* (15), 3553−3562.
(30) Spencer, M. T.; Prather, K. A. Using ATOFMS to determine OC/EC mass fractions in particles. *Aerosol Sci. Technol.* **2006**, *40* (8), 585−594.
(31) Toner, S. M.; Sodeman, D. A.; Prather, K. A. Single Particle Characterization of Ultrafine and Accumulation Mode Particles from Heavy Duty Diesel Vehicles Using Aerosol Time-of-Flight Mass Spectrometry. *Environ. Sci. Technol.* **2006**, *40* (12), 3912−3921.
(32) Gross, D. S.; Galli, M. E.; Silva, P. J.; Prather, K. A. Relative sensitivity factors for alkali metal and ammonium cations in single particle aerosol time-of-flight mass spectra. *Anal. Chem.* **2000**, *72* (2), 416−422.
(33) Moffet, R. C.; de Foy, B.; Molina, L. T.; Molina, M. J.; Prather, K. A. Measurement of ambient aerosols in northern Mexico City by single particle mass spectrometry. *Atmos. Chem. Phys.* **2008**, *8*, 4499−4516.
(34) Noble, C. A.; Prather, K. A. Real-time measurement of correlated size and composition profiles of individual atmospheric aerosol particles. *Environ. Sci. Technol.* **1996**, *30* (9), 2667−2680.
(35) Pratt, K. A.; Murphy, S. M.; Subramanian, R.; DeMott, P. J.; Kok, G. L.; Campos, T.; Rogers, D. C.; Prenni, A. J.; Heymsfield, A. J.; Seinfeld, J. H.; Prather, K. A. Flight-based chemical characterization of biomass burning aerosols within two prescribed burn smoke plumes. *Atmos. Chem. Phys.* **2011**, *11* (24), 12549−12565.
(36) Sullivan, R. C.; Prather, K. A. Investigations of the diurnal cycle and mixing state of oxalic acid in individual particles in Asian aerosol outflow. *Environ. Sci. Technol.* **2007**, *41* (23), 8062−8069.
(37) Yang, F.; Chen, H.; Wang, X. N.; Yang, X.; Du, J. F.; Chen, J. M. Single particle mass spectrometry of oxalic acid in ambient aerosols in Shanghai: Mixing state and formation mechanism. *Atmos. Environ.* **2009**, *43* (25), 3876−3882.
(38) Angelino, S.; Suess, D. T.; Prather, K. A. Formation of aerosol particles from reactions of secondary and tertiary alkylamines: Characterization by aerosol time-of-flight mass spectrometry. *Environ. Sci. Technol.* **2001**, *35* (15), 3130−3138.
(39) Kim, E.; Hopke, P. K.; Edgerton, E. S. Source identification of Atlanta aerosol by positive matrix factorization. *J. Air Waste Manage. Assoc.* **2003**, *53* (6), 731−739.
(40) Polissar, A. V.; Hopke, P. K.; Paatero, P. Atmospheric aerosol over Alaska - 2. Elemental composition and sources. *J. Geophys. Res.: Atmos.* **1998**, *103* (D15), 19045−19057.
(41) Reff, A.; Eberly, S. I.; Bhave, P. V. Receptor modeling of ambient particulate matter data using positive matrix factorization: Review of existing methods. *J. Air Waste Manage. Assoc.* **2007**, *57* (2), 146−154.
(42) Eatough, D. J.; Grover, B. D.; Woolwine, W. R.; Eatough, N. L.; Long, R.; Farber, R. Source apportionment of 1 h semi-continuous data during the 2005 Study of Organic Aerosols in Riverside (SOAR) using positive matrix factorization. *Atmos. Environ.* **2008**, *42* (11), 2706−2719.
(43) Healy, R. M.; Hellebust, S.; Kourtchev, I.; Allanic, A.; O'Connor, I. P.; Bell, J. M.; Healy, D. A.; Sodeau, J. R.; Wenger, J. C. Source apportionment of PM2.5 in Cork Harbour, Ireland using a combination of single particle mass spectrometry and quantitative semi-continuous measurements. *Atmos. Chem. Phys.* **2010**, *10* (19), 9593−9613.

(44) McGuire, M. L.; Jeong, C. H.; Slowik, J. G.; Chang, R. Y. W.; Corbin, J. C.; Lu, G.; Mihele, C.; Rehbein, P. J. G.; Sills, D. M. L.; Abbatt, J. P. D.; Brook, J. R.; Evans, G. J. Elucidating determinants of aerosol composition through particle-type-based receptor modeling. *Atmos. Chem. Phys.* **2011**, *11* (15), 8133−8155.
(45) Owega, S.; Khan, B. U. Z.; D'Souza, R.; Evans, G. J.; Fila, M.; Jervis, R. E. Receptor modeling of Toronto PM2.5 characterized by aerosol laser ablation mass spectrometry. *Environ. Sci. Technol.* **2004**, *38* (21), 5712−5720.
(46) *USEPA, EPA Positive Matrix Factorization (PMF) 3.0 Fundamentals & User Guide*; U. S. EPA Office of Research and Development: Washington, DC, 2008.
(47) Draxler, R. R.; Hess, G. D. An overview of the HYSPLIT 4 modelling system for trajectories, dispersion and deposition. *Aust. Meteorol. Mag.* **1998**, *47* (4), 295−308.
(48) Muhle, J.; Lueker, T. J.; Su, Y.; Miller, B. R.; Prather, K. A.; Weiss, R. F. Trace gas and particulate emissions from the 2003 southern California wildfires. *J. Geophys. Res.: Atmos.* **2007**, *112* (D3), DOI: 10.1029/2006JD007350.
(49) Phuleria, H. C.; Fine, P. M.; Zhu, Y. F.; Sioutas, C., Air quality impacts of the October 2003 Southern California wildfires. *J. Geophys. Res.: Atmos.* **2005**, *110*, (D7).
(50) Hossain, A. M. M. M.; Park, S.; Kim, J.-S.; Park, K. Volatility and mixing states of ultrafine particles from biomass burning. *J. Hazard. Mater.* **2012**, *205*, 189−197.
(51) Ramgolam, K.; Favez, O.; Cachier, H.; Gaudichet, A.; Marano, F.; Martinon, L.; Baeza-Squiban, A. Size-partitioning of an urban aerosol to identify particle determinants involved in the proinflammatory response induced in airway epithelial cells. *Part. Fibre Toxicol.* **2009**, *6*, 12.
(52) Schwartz, J.; Neas, L. M. Fine particles are more strongly associated than coarse particles with acute respiratory health effects in schoolchildren. *Epidemiology* **2000**, *11* (1), 6−10.
(53) Stoelzel, M.; Breitner, S.; Cyrys, J.; Pitz, M.; Woelke, G.; Kreyling, W.; Heinrich, J.; Wichmann, H. E.; Peters, A. Daily mortality and particulate matter in different size classes in Erfurt, Germany. *J. Exposure Sci. Environ. Epidemiol.* **2007**, *17* (5), 458−467.
(54) Guazzotti, S. A.; Whiteaker, J. R.; Suess, D.; Coffee, K. R.; Prather, K. A. Real-time measurements of the chemical composition of size-resolved particles during a Santa Ana wind episode, California USA. *Atmos. Environ.* **2001**, *35* (19), 3229−3240.
(55) Ault, A. P.; Moore, M. J. K.; Furutani, H. F.; Prather, K. A. Impact of Emissions from the Los Angeles Port Region on San Diego Air Quality during Regional Transport Events. *Environ. Sci. Technol.* **2009**, *43* (10), 3500−3506.
(56) Engelhart, G. J.; Hennigan, C. J.; Miracolo, M. A.; Robinson, A. L.; Pandis, S. N. Cloud condensation nuclei activity of fresh primary and aged biomass burning aerosol. *Atmos. Chem. Phys.* **2012**, *12* (15), 7285−7293.
(57) Silva, P. J. *Source profiling and apportionment of airborne particles: a new approach using aerosol time-of-flight mass spectrometry*; University of California Riverside: Riverside, CA, 2000.
(58) Pratt, K. A.; Prather, K. A. Real-Time, Single-Particle Volatility, Size, and Chemical Composition Measurements of Aged Urban Aerosols. *Environ. Sci. Technol.* **2009**, *43* (21), 8276−8282.
(59) Fiedler, V.; Arnold, F.; Ludmann, S.; Minikin, A.; Hamburger, T.; Pirjola, L.; Dornbrack, A.; Schlager, H. African biomass burning plumes over tc measurements and implications for H(2)SO(4) and HNO(3) mediated smoke particle activation. *Atmos. Chem. Phys.* **2011**, *11* (7), 3211−3225.
(60) Stelson, A. W.; Seinfeld, J. H. Relative-humidity and pH-dependence of the vapor-pressure of ammonium-nitrate nitric acid-solutions at 25-degrees-C. *Atmos. Environ.* **1982**, *16* (5), 993−1000.
(61) Stelson, A. W.; Seinfeld, J. H. Relative humidity and temperature dependence of the ammonium nitrate dissociation constant. *Atmos. Environ.* **1982**, *16* (5), 983−992.
(62) Lobert, J. M.; Scharffe, D. H.; Hao, W. M.; Kuhlbusch, T. A.; Seuwen, R.; Warneck, P. Experimental evaluation of biomass burning emissions: nitrogen and carbon containing compounds. In *Global Biomass Burning: atmospheric, climatic and biospheric implications*; Levine, J. S., Ed.; MIT Press: Cambridge, MA, 1991; pp 289−304.
(63) Streets, D. G.; Yarber, K. F.; Woo, J. H.; Carmichael, G. R. Biomass burning in Asia: Annual and seasonal estimates and atmospheric emissions. *Global Biogeochem. Cycles* **2003**, *17* (4), 20.
(64) Lefer, B. L.; Talbot, R. W.; Harriss, R. C.; Bradshaw, J. D.; Sandholm, S. T.; Olson, J. O.; Sachse, G. W.; Collins, J.; Shipham, M. A.; Blake, D. R.; Klemm, K. I.; Klemm, O.; Gorzelska, K.; Barrick, J. Enhancement of Acidic Gases in Biomass Burning Impacted Air Masses Over Cananda. *J. Geophys. Res.: Atmos.* **1994**, *99* (D1), 1721−1737.
(65) Talbot, R. W.; Bradshaw, J. D.; Sandholm, S. T.; Singh, H. B.; Sachse, G. W.; Collins, J.; Gregory, G. L.; Anderson, B.; Blake, D.; Barrick, J.; Browell, E. V.; Klemm, K. I.; Lefer, B. L.; Klemm, O.; Gorzelska, K.; Olson, J.; Herlth, D.; Ohara, D. Summertime distribution and relations of reactive odd nitrogen species and NOy in the troposphere over Canada. *J. Geophys. Res.: Atmos.* **1994**, *99* (D1), 1863−1885.
(66) Yokelson, R. J.; Susott, R.; Ward, D. E.; Reardon, J.; Griffith, D. W. T. Emissions from smoldering combustion of biomass measured by open-path Fourier transform infrared spectroscopy. *J. Geophys. Res.: Atmos.* **1997**, *102* (D15), 18865−18877.
(67) Song, C. H.; Ma, Y.; Orsini, D.; Kim, Y. P.; Weber, R. J. An Investigation into the Ionic Chemical Composition and Mixing State of Biomass Burning Particles Recorded During TRACE-P P3B Flight # 10. *J. Atmos. Chem.* **2005**, *51* (1), 43−64.
(68) Reid, J. S.; Hobbs, P. V.; Ferek, R. J.; Blake, D. R.; Martins, J. V.; Dunlap, M. R.; Liousse, C. Physical, chemical, and optical properties of regional hazes dominated by smoke in Brazil. *J. Geophys. Res.: Atmos.* **1998**, *103* (D24), 32059−32080.
(69) Saxena, P.; Seigneur, C. On the oxidation of SO2 to sulfate in atmospheric aerosols. *Atmos. Environ.* **1987**, *21* (4), 807−812.
(70) Laj, P.; Fuzzi, S.; Facchini, M. C.; Orsi, G.; Berner, A.; Kruisz, C.; Wobrock, W.; Hallberg, A.; Bower, K. N.; Gallagher, M. W.; Beswick, K. M.; Colvile, R. N.; Choularton, T. W.; Nason, P.; Jones, B. Experimental evidence for in-cloud production of aerosol sulphate. *Atmos. Environ.* **1997**, *31* (16), 2503−2514.
(71) Smith, S. J.; van Aardenne, J.; Klimont, Z.; Andres, R. J.; Volke, A.; Arias, S. D. Anthropogenic sulfur dioxide emissions: 1850−2005. *Atmos. Chem. Phys.* **2011**, *11* (3), 1101−1116.
(72) Pratt, K. A.; DeMott, P. J.; French, J. R.; Wang, Z.; Westphal, D. L.; Heymsfield, A. J.; Twohy, C. H.; Prenni, A. J.; Prather, K. A. In situ detection of biological particles in cloud ice-crystals. *Nat. Geosci.* **2009**, *2* (6), 397−400.
(73) Laskin, A.; Smith, J. S.; Laskin, J. Molecular Characterization of Nitrogen-Containing Organic Compounds in Biomass Burning Aerosols Using High-Resolution Mass Spectrometry. *Environ. Sci. Technol.* **2009**, *43* (10), 3764−3771.
(74) Ma, Y. L.; Hays, M. D. Thermal extraction-two-dimensional gas chromatography-mass spectrometry with heart-cutting for nitrogen heterocyclics in biomass burning aerosols. *J. Chromatogr., A* **2008**, *1200* (2), 228−234.
(75) Mace, K. A.; Artaxo, P.; Duce, R. A. Water-soluble organic nitrogen in Amazon Basin aerosols during the dry (biomass burning) and wet seasons. *J. Geophys. Res.: Atmos.* **2003**, *108* (D16), 10.
(76) Roberts, J. M.; Veres, P. R.; Cochran, A. K.; Warneke, C.; Burling, I. R.; Yokelson, R. J.; Lerner, B.; Gilman, J. B.; Kuster, W. C.; Fall, R.; de Gouw, J. Isocyanic acid in the atmosphere and its possible link to smoke-related health effects. *Proc. Natl. Acad. Sci. U. S. A.* **2011**, *108* (22), 8966−8971.
(77) Simpson, I. J.; Akagi, S. K.; Barletta, B.; Blake, N. J.; Choi, Y.; Diskin, G. S.; Fried, A.; Fuelberg, H. E.; Meinardi, S.; Rowland, F. S.; Vay, S. A.; Weinheimer, A. J.; Wennberg, P. O.; Wiebring, P.; Wisthaler, A.; Yang, M.; Yokelson, R. J.; Blake, D. R. Boreal forest fire emissions in fresh Canadian smoke plumes: C(1)-C(10) volatile organic compounds (VOCs), CO(2), CO, NO(2), NO, HCN and CH(3)CN. *Atmos. Chem. Phys.* **2011**, *11* (13), 6445−6463.
(78) Veres, P.; Roberts, J. M.; Burling, I. R.; Warneke, C.; de Gouw, J.; Yokelson, R. J. Measurements of gas-phase inorganic and organic

acids from biomass fires by negative-ion proton-transfer chemical-ionization mass spectrometry. *J. Geophys. Res.: Atmos.* **2010**, *115*, 15.
(79) Yokelson, R.; Crounse, J. D.; DeCarlo, P.; Karl, T.; Urbanski, S.; Atlas, E.; Campos, T.; Shinozuka, Y.; Kapustin, V. N.; Clarke, A. D.; Weinheimer, A.; Knapp, D. J.; Montzka, D. D.; Holloway, J.; Weibring, P.; Flocke, F.; Zheng, W.; Toohey, D.; Wennberg, P. O.; Wiedinmyer, C.; Mauldin, L.; Freid, A.; Richter, D.; Walega, J.; Jimenez, J. L.; Adachi, K.; Buseck, P. R.; Hall, S. R.; Shetter, R. Emissions from biomass burning in the Yucatan. *Atmos. Chem. Phys.* **2009**, *9*, 5785−5812.
(80) Legrand, M.; Preunkert, S.; Oliveira, T.; Pio, C. A.; Hammer, S.; Gelencser, A.; Kasper-Giebl, A.; Laj, P. Origin of C-2-C-5 dicarboxylic acids in the European atmosphere inferred from year-round aerosol study conducted at a west-east transect. *J. Geophys. Res.: Atmos.* **2007**, *112* (D23), 14.
(81) Miyazaki, Y.; Aggarwal, S. G.; Singh, K.; Gupta, P. K.; Kawamura, K. Dicarboxylic acids and water-soluble organic carbon in aerosols in New Delhi, India, in winter: Characteristics and formation processes. *J. Geophys. Res.: Atmos.* **2009**, *114*, 12.
(82) Rehbein, P. J. G.; Jeong, C. H.; McGuire, M. L.; Yao, X. H.; Corbin, J. C.; Evans, G. J. Cloud and Fog Processing Enhanced Gas-to-Particle Partitioning of Trimethylamine. *Environ. Sci. Technol.* **2011**, *45* (10), 4346−4352.
(83) Narukawa, M.; Kawamura, K.; Takeuchi, N.; Nakajima, T. Distribution of dicarboxylic acids and carbon isotopic compositions in aerosols from 1997 Indonesian forest fires. *Geophys. Res. Lett.* **1999**, *26* (20), 3101−3104.
(84) Timonen, H.; Aurela, M.; Carbone, S.; Saarnio, K.; Saarikoski, S.; Makela, T.; Kulmala, M.; Kerminen, V. M.; Worsnop, D. R.; Hillamo, R. High time-resolution chemical characterization of the water-soluble fraction of ambient aerosols with PILS-TOC-IC and AMS. *Atmos. Meas. Tech.* **2010**, *3* (4), 1063−1074.
(85) Noblitt, S. D.; Lewis, G. S.; Liu, Y.; Hering, S. V.; Collett, J. L.; Henry, C. S. Interfacing Microchip Electrophoresis to a Growth Tube Particle Collector for Semicontinuous Monitoring of Aerosol Composition. *Anal. Chem.* **2009**, *81* (24), 10029−10037.
(86) Worton, D. R.; Kreisberg, N. M.; Isaacman, G.; Teng, A. P.; McNeish, C.; Gorecki, T.; Hering, S. V.; Goldstein, A. H. Thermal Desorption Comprehensive Two-Dimensional Gas Chromatography: An Improved Instrument for In-Situ Speciated Measurements of Organic Aerosols. *Aerosol Sci. Technol.* **2012**, *46* (4), 380−393.
(87) Zauscher, M. D.; Moore, M. J. K.; Lewis, G. S.; Hering, S. V.; Prather, K. A. Approach for Measuring the Chemistry of Individual Particles in the Size Range Critical for Cloud Formation. *Anal. Chem.* **2011**, *83* (6), 2271−2278.